Coral Reefs
https://doi.org/10.1007/s00338-025-02675-0

RESEARCH

Sensitivity of reef-relevant ocean color phenomena to satellite data resolution

Jessica N. Perelman[1,2] · Hui Shi[1,2] · Ryan R. Rykaczewski[2,3] · Justin J. Suca[3] · Ryan A. Vandermeulen[4] · Dax Matthews[1,2]

Received: 28 September 2024 / Accepted: 25 April 2025

Abstract Satellite ocean color measurements are a valuable tool for evaluating water quality parameters relevant to coral reef habitats. However, low earth orbiting satellites offer a limited number of observations for detecting episodic, extreme events to which coral reefs are sensitive, and the spatial resolution of most sensors is too coarse for fine scale processes in optically shallow nearshore environments. Here, we assess whether high-resolution satellite ocean color measurements from the first geostationary satellite ocean color sensor (GOCI) can improve our understanding of coral reef habitat conditions and monitoring capabilities for potential reef changes. Using ten years (2011–2021) of GOCI ocean color measured eight times per day at a spatial resolution of 500 m around the Okinawa Prefecture region, we found that the high-resolution grid significantly increased retention of coastal areas where waters were otherwise masked at coarser resolutions (i.e., 4 km) to avoid optical reflectance in shallow waters. Contrary to expectation, we found that the often highly correlated variables chlorophyll-*a* and K_d490 did not notably decouple at higher spatiotemporal resolutions. However, the ability to detect episodic, extreme chlorophyll blooms increased significantly with increasing spatiotemporal resolution and the locations of these events became much more refined at higher resolutions. Finally, the high-resolution chlorophyll-*a* data captured up to 770 episodic events that were missed by the commonly used 4-km 8-day resolution data in any given grid cell around Okinawa across the 10-year period. High-resolution ocean color data can therefore enable us to assign more reliable risk to coral reef tracts that could be affected by frequent episodic events, and allows us to assess the persistence of such events in waters much closer to coastal habitat.

Keywords Geostationary ocean color · Coral reef · Satellite · Chlorophyll-a · Episodic events

Introduction

The world's coral reefs are unique natural resources, providing habitat for about 25% of all known marine species (Hoegh-Guldberg et al. 2017) including over 4000 species of fish (EPA 2022). However, the clear, clean waters that are necessary for these systems to thrive are subject to threats from both changing climate conditions and from human development. Human populations have long been concentrated along coasts, but the impacts of human activities on coastal ecosystems are particularly evident on tropical islands where 90% of people live along the shoreline (Andrew et al. 2019), creating additional pressures on coral reef ecosystems from land-based pollution and erosion (Bryant et al. 2001). Efforts to assess the health of coral reef environments and the impacts of human development and changing climate would benefit from

Supplementary Information The online version contains supplementary material available at https://doi.org/10.1007/s00338-025-02675-0.

✉ Jessica N. Perelman
jessica.perelman@noaa.gov

1 Cooperative Institute for Marine and Atmospheric Research, University of Hawaii, 1000 Pope Road, Honolulu, HI 96822, USA

2 Pacific Islands Fisheries Science Center, National Marine Fisheries Service, 1845 Wasp Boulevard, Honolulu, HI 96818, USA

3 Department of Oceanography, University of Hawai'i at Mānoa, 1000 Pope Rd, Honolulu, HI 96822, USA

4 Office of Science and Technology, National Marine Fisheries Service, Silver Spring, MD, USA

Published online: 30 May 2025

increased observational capabilities, particularly those informing metrics of water quality from optical proxies (Devlin et al. 2015). Here, we analyze the sensitivity of remotely sensed assessments of the optical environment to varying spatial and temporal data resolutions with the objective of demonstrating the potential value of future satellite missions to reef-dependent communities.

Coral reef environments rely on specific conditions, one of them being relatively shallow waters that are typically confined to a narrow coastal band (i.e., a fringing reef). Unfortunately, the shallow and coastal nature of these systems make them challenging to assess by satellites, as the spatial resolutions of most optical sensors that can view a given location at a daily cadence are too coarse for the collection of data on fine scales appropriate for the nearshore environment (Bissett et al. 2004). In these nearshore waters where coral reefs inhabit, the optical properties of the water column can be influenced by non-algal particulate matter and colored dissolved organic matter (CDOM) that do not necessarily co-vary with respect to phytoplankton abundance (IOCCG 2000), therefore requiring specific ocean color algorithms to effectively derive accurate remotely sensed water quality parameters (Hedley et al. 2016). Additionally, most coral reef environments are in optically shallow water, where the reflectance of the sea floor and suspended sediment may affect the light received by satellite sensors and cause data quality issues in ocean color measurements (McKinna and Werdell 2018).

One common, but unsatisfying approach to resolve the data quality issue is to remove data pixels that are within (or partially within) shallow water regions (Gove et al. 2013). With the removal of shallow water grid cells, the grid cells that lie adjacent to the mask boundary are typically the ones used as a proxy to evaluate productivity and turbidity around shallow reef habitats (Couch et al. 2023; Winston et al. 2022). However, coral reef systems themselves influence the water quality and spectral composition of light on the reef ecosystem and result in optical properties in reef waters that differ substantially from nearby offshore optically deep waters (Russell et al. 2019). Although water quality will undoubtedly vary at fine scales within a coral reef environment, detecting offshore productivity along reef margins may help determine whether there are (relatively) large-scale events that affect water quality enough to extend offshore. While developing ocean color algorithms for optically complex and optically shallow waters remains an active area of research (Barnes et al. 2013; Brando et al. 2012; Doerffer and Schiller 2007; Lee and Carder 2002; McKinna et al. 2015; Werdell et al. 2013), using data of higher spatial resolution could greatly decrease the fraction of coastal habitats influenced by optically shallow water data quality issues.

Coral reefs are sensitive to episodic, extreme events (e.g., marine heatwaves, waste water pollution, urban runoff, etc.). However, effectively monitoring and detecting these changes can be challenging with limited in situ observations. Satellite imagery is a power tool to monitor and contextualize these events at more synoptic scales, but the technological limitations of satellites can also make it challenging to resolve the transient nature of coastal processes. Most optical sensors are onboard polar-orbiting satellites [e.g., the Moderate Resolution Imaging Spectroradiometer (MODIS) onboard the Terra and Aqua satellites and the Visible Infrared Imaging Radiometer Suite (VIIRS) onboard the Suomi National Polar-Orbiting Partnership (Suomi NPP) spacecraft], and the ocean color satellite images are available at the daily time scale. However, a daily overpass does not equate to daily data retrievals, as these images are often obscured by cloud cover (Geiger et al. 2021; Gholizadeh et al. 2016). On a daily basis, a satellite sensor viewing the Earth will only be able to image 15–20% of the global oceans (IOCCG 1999). In order to reduce data gaps and generate a more consistent time series, it is common practice to aggregate satellite data over larger space and time scales (4 km, 8 day average), at the expense of potentially smoothing out the small-scale, episodic changes in water quality that can have ecological ramifications. High temporal resolution satellite observations can improve the monitoring and detection capabilities of extreme events as well as more accurately capture their location in coastal regions.

Notably, phytoplankton biomass can be naturally enhanced by the presence of the islands or atolls–an observation termed the "island mass effect" (Gove et al. 2016). Understanding the relationship between turbidity and chlorophyll-*a* and their influence on the abundance of reef fishes and coral reef recovery is important. High empirical correlations exist between chlorophyll-a and light attenuation (K_d490) in oceanic waters where the light extinction is largely driven by phytoplankton biomass, or so-called Case 1 waters (Morel et al. 2007). The rate at which light is attenuated with depth is represented by the diffuse attenuation coefficient at 490 nm (K_d490), which is directly related to the amount of scattering particles in the water column and turbidity. Ongoing studies comparing the occurrence of reef fishes in the Main Hawaiian Islands have shown negative relationships with chlorophyll-a (Suca et al., in prep.). This runs counter to the general expectation that higher primary productivity is beneficial to fisheries productivity (Link and Watson 2019; McClanahan et al. 2019). These results are likely due to the substantial contribution of benthic algae and invertebrates to reef-based food webs (Choat et al. 2002) and the conflation of turbid waters (which include turbidity caused by human land use) with chlorophyll-a concentration. In instances where light attenuation is impacted by

other, land-based constituents such as suspended particulate matter and/or chromophoric dissolved organic matter, the relative contribution from chlorophyll-a can be significantly diminished (Abdelrhman 2017). Higher spatiotemporal resolution data of both turbidity (proxied by K_d490) and chlorophyll-a can potentially allow for differentiation of acute, small-scale increases in these parameters from river outflow or human land use compared to more persistent, broader-scale increases in chlorophyll associated with natural conditions like the island mass effect or oceanic processes.

In June 2010, South Korea launched the first geostationary ocean color sensor, the Geostationary Ocean Color Imager (GOCI; Choi et al. 2012), onboard the Communication, Ocean, and Meteorological Satellite (COMS). From April 2011 to March 2021, GOCI provided hourly imagery in six spectral bands (6 in the visible, and 2 in the near-infrared) at a spatial resolution of 500 m. This level temporal, spatial, and spectral sampling allowed GOCI to effectively monitor small-scale ocean phenomena, such as tide-induced sediment re-suspension, diurnal variation of ocean optical and biogeochemical properties, and horizontal advection of river discharge (Wang et al. 2013).

GOCI imagery demonstrated potential benefits that frequent, high-resolution ocean color monitoring could provide worldwide. Future missions, such as NOAA's Ocean Color (OCX) instrument onboard the next generation Geostationary Extended Observations (GeoXO) satellite series, will continue this work. In the following, we explore how future geostationary ocean color imagery may improve our understanding of reef conditions by investigating how coral reef monitoring capabilities are affected by the temporal and spatial resolution of the ocean color imagery.

For this study, we focus on the Ryukyu Island Arc, which sits within the GOCI observation domain and is home to diverse fringing reefs. The Kuroshio Current runs northeast through the Ryukyu Islands, bringing warm oligotrophic waters that support coral reef habitats across this region (Asanuma et al. 2014; Koba 1992). Here, with the high spatial–temporal measurements from the GOCI sensor, we assess the sensitivity of detecting satellite-derived ocean phenomena around these coral reef habitats to changes in data resolution. The goal of this work is to explore ways in which geostationary satellite data could improve our understanding of reef conditions in areas where in situ measurements are limited, and to evaluate new monitoring capabilities for potential reef changes with the implementation of geostationary ocean color satellite sensors. We focus on two main areas regarding the utility of high-resolution satellite data: (1) the ability to better distinguish differences between ocean color variables measured in nearshore habitats that are used as water quality indices, (2) the ability to detect extreme, episodic events to evaluate the impacts of runoff or pollution events near reef habitats.

Data

Ocean color

GOCI-derived ocean color data are collaboratively developed by the NOAA Center for Satellite Applications (STAR) and Korea Institute of Ocean Science and Technology. They are produced using the Multi-Sensor Level-1 to Level-2 (MSL12) ocean color data processing with the Near-Infra-Red (NIR; (Gordon and Wang 1994) and the NIR reflectance correction algorithm (Jiang and Wang 2014). GOCI-derived ocean color data have been found to compare well with in situ data (Wang et al. 2013) as well as those from VIIRS measurements (Wang et al. 2023). For these analyses we used ten years of Level-3 ocean color data (2011–2021) around the Okinawa Prefecture region (Fig. 1) provided by NOAA/NESDIS/STAR with a spatial and temporal resolution of 500 m and 8× per day, respectively. Level-3 GOCI ocean color data is masked for straylight effects from land and clouds (Wang and Shi 2006) meaning that some pixels very close to shore have been removed.

Bathymetry

We explored several high-resolution bathymetry datasets and found that the STRM15+ v2.6 (05/2024) product identifies shallow reefs around Okinawa most closely to those represented in Google Earth satellite imagery. This dataset incorporates shipboard soundings from near Japan (Tozer 2019) and uses the global locations of warm coral reefs as a proxy for shallow bathymetry (UNEP-WCMC 2021). Thus, while it is not a perfect match to the satellite imagery presented in Google Earth, we feel that this bathymetry dataset offers the most accurate representation of seafloor depths for the purposes of masking shallow waters (less than ~30 m) in our study.

Methods

Simulating ocean color grids

In order to present a modeling study that focuses on data resolution and hold all other variables that could differ between satellite sensors and processing steps constant, we chose to simulate spatiotemporally coarsened grids to replicate existing satellite ocean color configurations (such as VIIRS and SeaWIFS) rather than using coarser data from these existing products. After downloading and cropping

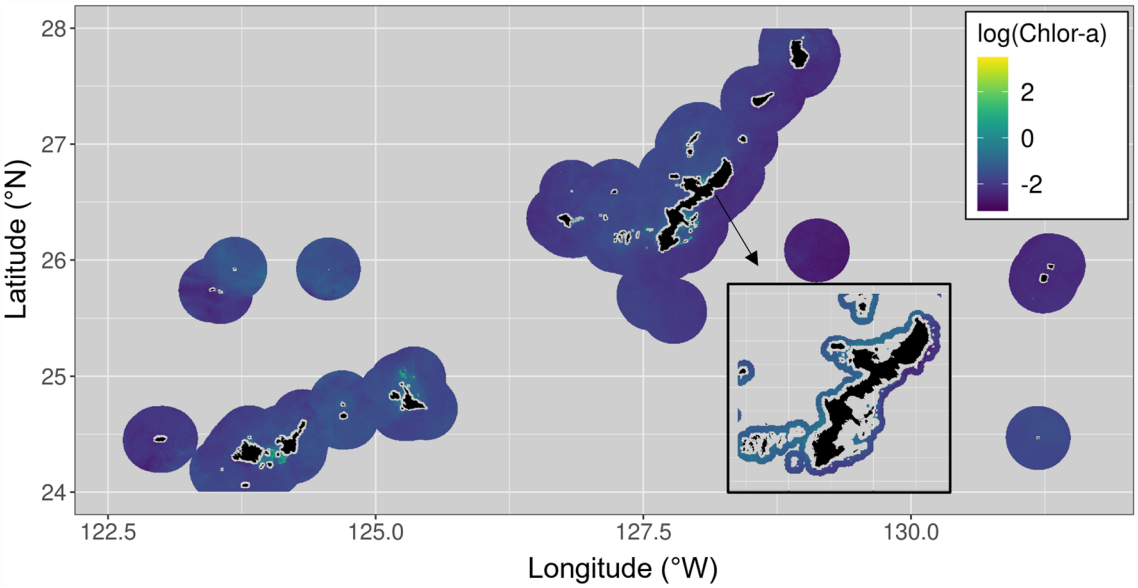

Fig. 1 Map of Okinawa Prefecture region showing GOCI Level-3 mean chlorophyll-a concentration (mg m^{-3}) in March 2021 prior to shallow water masking. Inset shows chlorophyll-a concentration around Okinawa Island after the removal of shallow water grid cells

the full-resolution (500 m) GOCI data files, we simulated coarser 1-day resolution files at 750 m and 4 km by first extracting the measurement closest to noon. These values were used as the "daily" estimates for generating coarser resolution grids. We then simulated new grids to replicate existing satellite ocean color spatial resolutions at 750 m and 4 km by aggregating and averaging the original 500-m pixels. Since each 750-m resolution grid cell represents 2.25 GOCI cells, we first regridded the 500-m cells to 375 m using bilinear interpolation before aggregating and averaging those cells to 750 m. The resulting chlorophyll and K_d490 values did not differ significantly when regridding with bilinear or nearest neighbor interpolation and did not change any of the results. For the grid simulation step, we added a "cloud mask" similarly to other satellite ocean color products by setting a minimum threshold of 50%. With this threshold, a coarsened pixel would only receive a value at a given time step if at least 50% of high-resolution pixels comprising that coarsened pixel had a non-missing value. In other words, any coarsened pixel would only be attributed a value if enough of the area comprising it contained data.

After simulating spatially coarsened grids, we masked shallow water pixels to remove any potential contamination of pixels by seafloor reflectance in shallow waters that is often an issue in coral reef environments (e.g., Maina 2011; Reichstetter et al. 2015). We used the 30-m isobath plus an additional ½ diagonal pixel distance perpendicular to this contour as the mask boundary at each spatial resolution following the methods of Gove et al. (2013). All pixels shallower than this boundary were removed from each grid and excluded from analyses (e.g., Fig. 1).

Finally, we simulated coarsened temporal resolution data by averaging each grid cell across 8-day and monthly windows from the daily resolution at 500 m, 750 m, and 4 km. We focused on the ocean color pixels closest to coral reef habitat along the coastal shallow water boundaries of Okinawa that encompass similar spatial areas for the analyses that follow. We thus focused on all pixels adjacent to the mask boundary at 4 km, the 5 pixels out perpendicular to the mask boundary at 750 m, and the 8 pixels out perpendicular to the mask boundary at 500 m. The resulting grid configurations that were used for subsequent analyses are presented in Table 1.

Table 1 Satellite ocean color grid configurations simulated from GOCI

Configuration	Spatial resolution	Temporal resolution
Coarse (e.g., SeaWIFS)	4 km	Daily
		8-day
		Monthly
Moderate (e.g., VIIRS)	750 m	Daily
		8-day
		Monthly
Full GOCI resolution	500 m	8× per day
		Daily
		8-day
		Monthly

Comparing water quality indices across spatiotemporal scales

To evaluate the relationships between chlorophyll (chlor-*a*) and K_d490 derived from satellite ocean color data across spatial and temporal scales, we first normalized their distributions via log transformation. We then extracted the full 10-year time series of these variables for each individual grid cell at every spatiotemporal scale and ran a linear regression between the two variables for every grid cell at every resolution. We assessed the correlation coefficients (r), slopes, and p-values to identify changes in the association between chlor-*a* and K_d490 with increasing spatial and temporal resolution. To assess whether changes in correlation values across scales were significant, we used Kruskal–Wallis rank-sum tests followed by Dunn tests for multiple pairwise comparisons. We further evaluated how these relationships change seasonally and with increasing distance from the coastline.

Detecting episodic events across spatiotemporal scales

We focused on the region immediately surrounding Okinawa Island to evaluate differences in the ability to detect episodic or extreme chlor-*a* events with increasing spatiotemporal resolution ocean color data. Episodic events were defined as a chlor-*a* value greater than a threshold of two standard deviations above the monthly mean value for each month to account for seasonality, therefore enabling us to distinguish sudden events such as typhoons or heavy rainfall from normal seasonal variations. We used the coarsest resolution data (4 km monthly chlor-*a*) to define these thresholds for defining events across all spatiotemporal resolutions for consistency. Thus, at a given time point, any grid cell with a chlor-a concentration above this threshold value was considered an episodic event. In order to avoid over-counting events that spanned multiple timepoints at the finest temporal resolution (8× per day), episodic events were separated by at least eight time points such that a maximum of one event could occur per day. We subsequently evaluated and mapped the total number of episodic events detected over the 10-year period within each grid cell at every resolution.

In addition, we identified the number of episodic events that were missed at the 4-km 8-day resolution data (a commonly used product for coastal habitats) but that were captured with the 500-m 8×-per-day resolution data. To do this, we identified instances where no anomalous event was detected at the 4-km 8-day scale, but was positively detected from any point within the corresponding 500-m, 8×-per-day sub-grid over the same time period. If any 500-m grid cell experienced an event at an 8×-per-day time step, then the entire 4-km grid cell was categorized as an extreme event for that time step. Unique events were summed for the entire 8-day window (events spanning multiple 8×/day time steps were only counted once). Only events during 8-day time windows where no events were detected at the 4-km scale were considered to be "missed" events.

Results

Coastal area and days gained from higher spatiotemporal resolution ocean color grid

We compared several satellite ocean color spatial coverage metrics along the coastal Okinawa region between the commonly used 4-km grid and the high-resolution GOCI 500-m grid. Considering only the grid cells adjacent to the shallow water reflectance boundary (i.e., 30-m isobath + ½ diagonal grid pixel), we found that the innermost high-resolution grid cells extend 3.8 km closer to the shoreline on average compared to the coarser resolution (4 km pixels averaged 6.2 km from the shore while 500-m pixels averaged 2.3 km from the shore; Fig. 2). Further, there was a 71% increase (1280 km^2) in area coverage by the 500-m grid inside of the 4-km grid boundary along nearshore regions most relevant for assessing coral reef habitats (i.e., the shallow water boundary). We further found that the coastal Okinawa grid cells from the full 8×-per-day resolution GOCI data had a median value of 1390 days with observations, compared to just 600 days at the once daily resolution where observations were taken nearest to noon. Seasonally, we found that highest

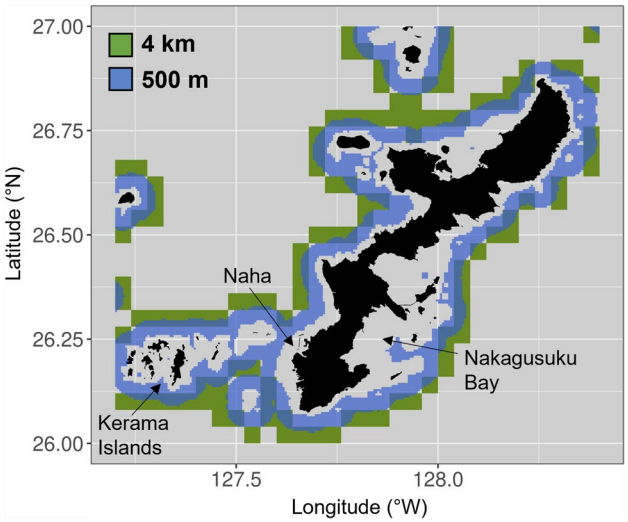

Fig. 2 Increased spatial coverage along Okinawa's coastal habitat from the 500-m GOCI ocean color grid (blue) in comparison with a 4-km grid (green). Grid cells are shown for the areas immediately adjacent to the shallow water reflectance boundary (30-m isobath + ½ diagonal pixel boundary)

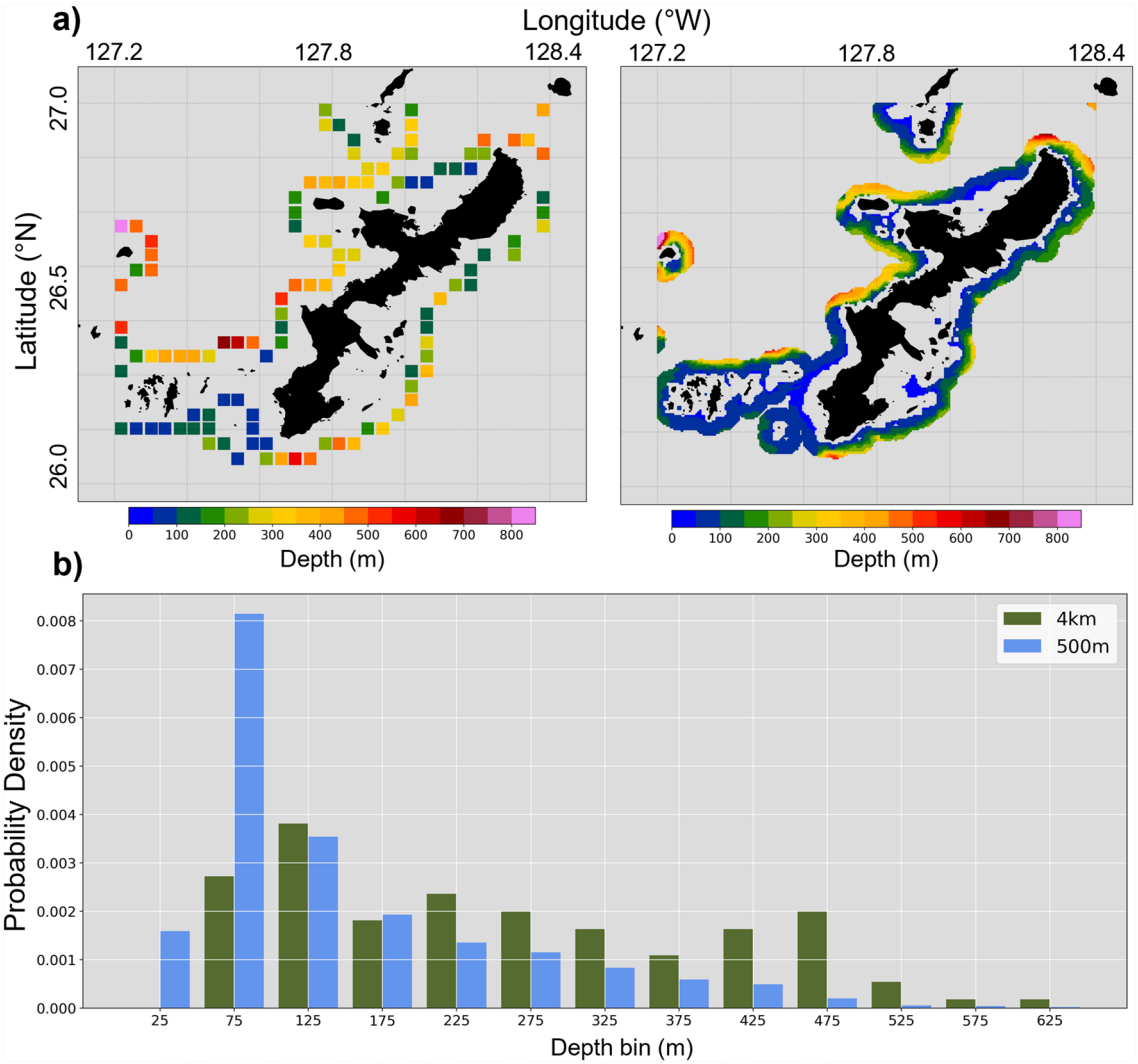

Fig. 3 Increased coverage of shallow water areas along Okinawa's coastal habitat from the high-resolution GOCI ocean color grid. **a** Maps showing water depth in grid cells adjacent to the shallow water reflectance boundary at 4 km and 500 m. **b** Probability density of coastal ocean color grid cells across depth bins at 4-km (green) and 500-m (blue) resolution

resolution GOCI grid cells had up to ~ 4× more observations during the summer months compared to the winter months across the timeseries (Supplementary Figure S1).

The improved spatial coverage offered by the high-resolution GOCI grid has the greatest impact on the data collected from waters shallower than 100 m (Fig. 3). The shallowest 4-km grid cell along the shallow water reflectance boundary is 57 m depth, while the shallowest 500-m grid cell is 31 m depth. Thus, the 500-m grid provides satellite ocean color data coverage closer to potential coral reef habitat in nearly all waters surrounding Okinawa Island, compared to a 4-km grid that provides data for waters of potential coral reef habitat that are confined largely to a region southwest of Okinawa.

Comparison of water quality indices across spatiotemporal scales

We found that the correlations between chlor-*a* and K_d490 across the full 10-year time series were generally high and grew significantly stronger at higher spatial resolution grid configurations (Kruskal–Wallis and Dunn test, $p < 0.001$; Fig. 4). We further found that the slopes of the relationships between chlor-*a* and K_d490 (i.e., the amount that K_d490 increased with each step increase of chlor-*a*) were significantly lower ($p < 0.001$) and had a narrower spread at the 4 km spatial scale compared to higher resolutions.

Our results showed that the correlations between chlor-*a* and K_d490 across the full 10-year time series were

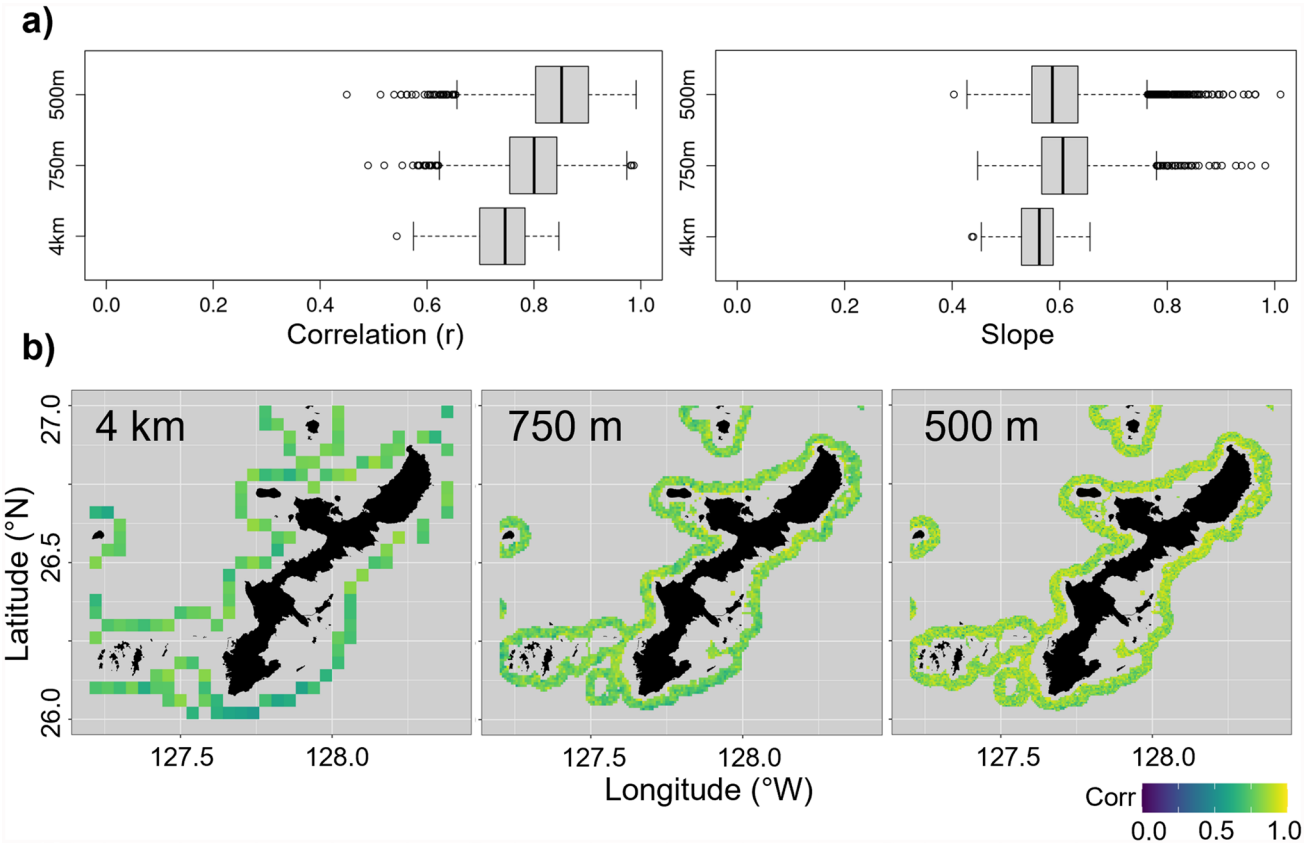

Fig. 4 Changes in coastal chlor-*a* and K_d490 correlations (2011–2021) across spatial scales at the daily temporal resolution. **a** Boxplots showing the range of cell-by-cell correlations and slopes values across the entire Okinawa Prefecture region at coarse (4 km), moderate (750 m), and full (500 m) resolution grid configurations. **b** Cell-by-cell correlation values mapped around nearshore Okinawa Island at coarse, moderate, and full-resolution grid configurations

significantly different across all temporal scales at the full 500-m spatial resolution (Kruskal–Wallis and Dunn test, $p < 0.001$), with an increasing trend from the monthly scale to the daily scale and a slight decrease from the daily to the 8×/day scale (Fig. 5). The spread of correlation values and slopes of the relationships between chlor-*a* and K_d490 were narrowest at the 8×/day scale.

We explored whether the trends in correlations between chlor-*a* and K_d490 were sensitive to seasonality and found that every season followed the same general trends: increasing correlations at finer spatial scales and slightly lower correlations at the 8×/day time scale (Supplementary Figure S2, S3). Further, we evaluated whether correlations at the grid cell level were sensitive to the distance from the coastline and found a very weak but significant decrease in correlations at greater distances from shore ($p < 0.001$; Supplementary Fig. S4). Finally, we evaluated whether correlations between chlor-*a* and K_d490 at the 500 m, 8×/day grid resolution were sensitive to the timing of extreme, episodic chlor-*a* events and found a small but significant decrease in correlations during non-event timepoints (Supplementary Fig. S5).

Detection of episodic, extreme events in coastal Okinawa is sensitive to data resolution

Our results indicate that the number of extreme chlorophyll events detected from satellite ocean color data increased with increasing spatiotemporal resolution (Figs. 6, 7) during both summer and winter months (Kruskal–Wallis rank-sum test, $p < 0.001$). The number of events increased most notably at 8×/day for both summer (median = 96, Wilcoxon rank-sum test, $p < 0.001$) and winter (median = 36, Wilcoxon rank-sum test, $p < 0.001$). At each spatiotemporal grid resolution, the number of events detected was significantly greater during the summer compared to winter (Kruskal–Wallis rank-sum test, $0 < p < 0.03$). Compared to the commonly used 4 km 8-day grid configuration, the full-resolution GOCI grid detected roughly 10 times more events that were spaced at least a day apart during summer and winter.

The locations of extreme chlor-*a* event hotspots around coastal Okinawa also changed and became more refined at higher spatial and temporal resolution grid configurations (Fig. 7). At coarse resolutions (e.g., daily/8-day 4 km) grid

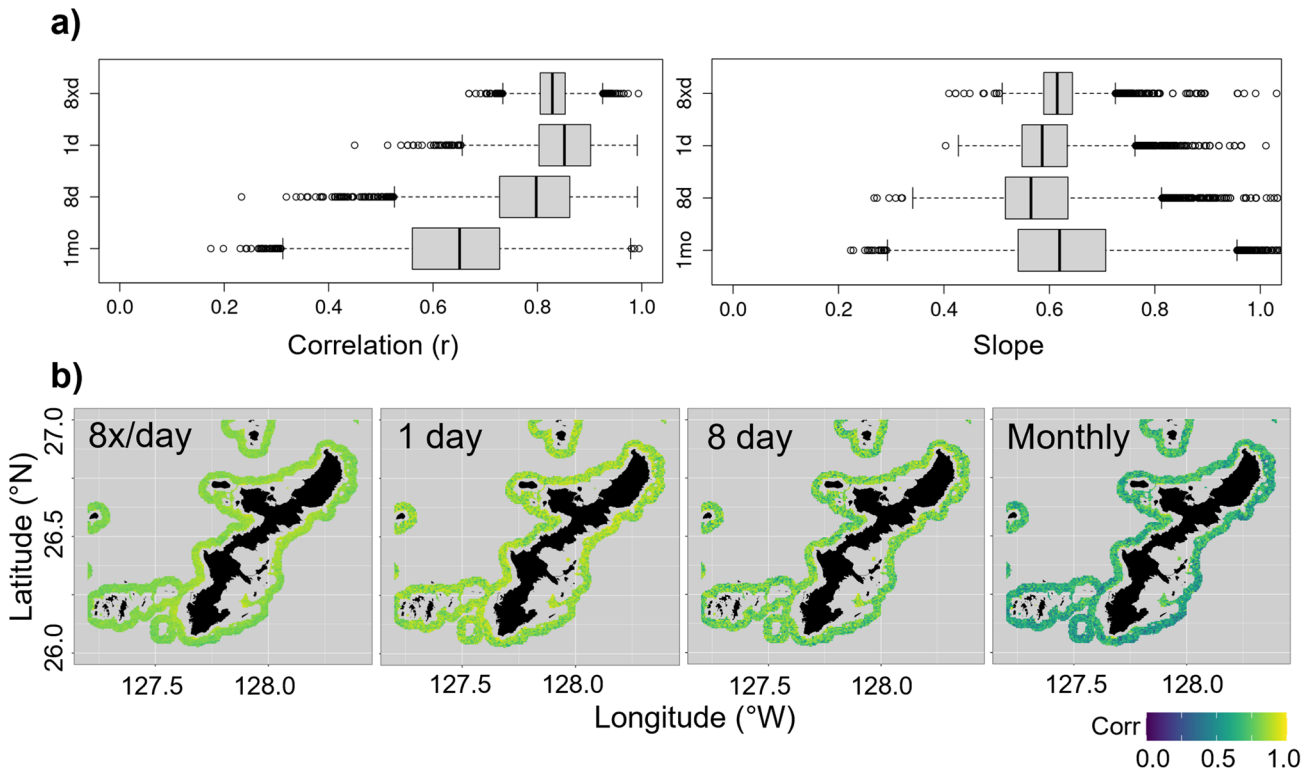

Fig. 5 Changes in coastal chlor-*a* and K_d490 correlations (2011–2021) across temporal scales at the full 500-m grid resolution. **a** Boxplots showing the range of cell-by-cell correlations and slopes values across the entire Okinawa Prefecture region at monthly, 8-day, daily, and 8×/day time configurations. **b** Cell-by-cell correlation values mapped around nearshore Okinawa Island at monthly, 8-day, daily, and 8×/day resolution grid configurations

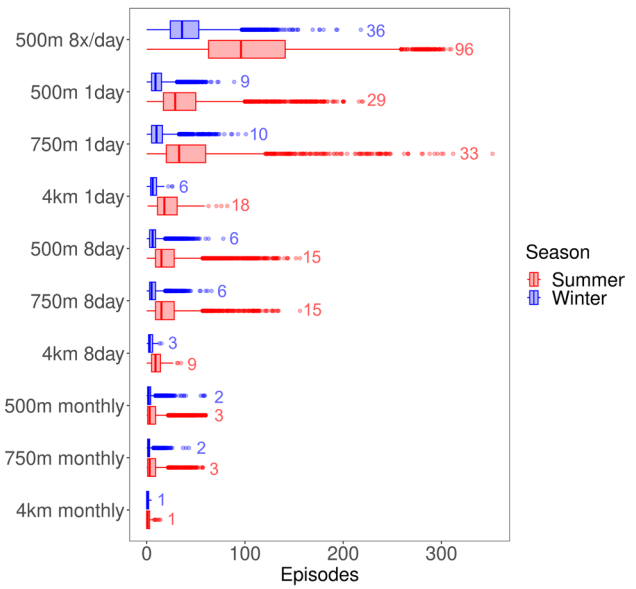

Fig. 6 Boxplots showing the range of episodic chlor-*a* events detected for each grid cell at every spatial and temporal resolution grid configuration across the 10-year timeseries (2011–2021) by season. Numbers indicate the median number of episodic events detected at a given grid configuration for summer (red) and winter (blue)

configurations, hotspots were primarily located between the Kerama Islands and southwest Okinawa. However, these hotspots became less pronounced at higher spatiotemporal resolution grid configurations, and extreme chlor-*a* event hotspots became particularly well defined within and around the outlet of Nakagusuku Bay and along the southwest coast between the prefectural capital of Naha and the Kerema Islands. These areas did not change substantially between the 750-m and 500-m daily and 8×/per-day grid configurations.

We identified the total number of episodic chlor-*a* events that were missed at the commonly used 8-day 4-km resolution grid configuration but that were captured by the full 8×/day 500-m resolution GOCI data (Fig. 8). The highest resolution chlor-*a* data captured up to 770 episodic events that were missed by the commonly used 4 km 8-day resolution in any given grid cell around in the Okinawa Island region. The area where the most events were missed was just south of the Kerama Islands to the southwest of Okinawa.

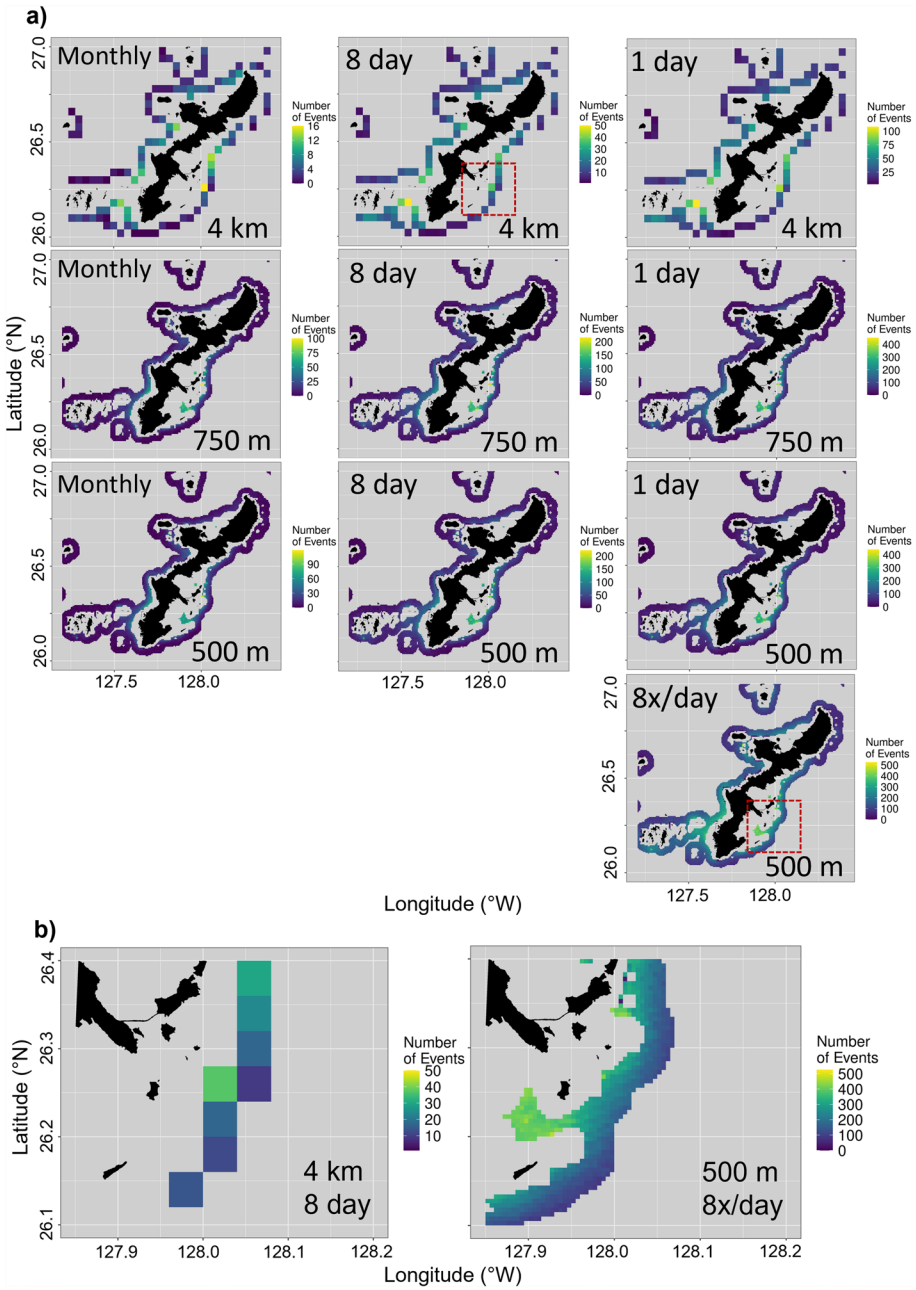

Fig. 7 **a** Number of episodic chlor-*a* events across the 10-year time series (2011–2021) within each grid cell mapped across coastal Okinawa at every spatial and temporal resolution grid configuration. Red boxes indicate zoomed in area around Nakagusuku Bay in (**b**)

Discussion

Enhanced coastal proximity of high-resolution satellite data near coral reef habitat

The distance between the coastline and usable ocean color data is much closer with the 500-m resolution data, only about 1/3rd of the distance in comparison to the 4-km data. Thus, we gain 71% more spatial coverage along the "shallow water mask" boundary that provides substantially more data in regions most relevant for assessing habitats along the deeper margins and immediately offshore of coral reefs. While this work utilized a static 30-m isobath (+ ½ diagonal grid cell) mask to avoid bottom reflectance contamination, additional nearshore coverage may be gained using a dynamically determined optically shallow water mask for ocean color (McKinna and Werdell 2018). We also gain around 2.3 × more days with observations around coastal Okinawa with the availability of geostationary data collecting measurements 8×-per-day as compared to once daily measurements. This is in line with other observations where, on average, daily composites from GOCI consistently retrieve > 2× spatial coverage relative to VIIRS for the sensor's entire field of regard

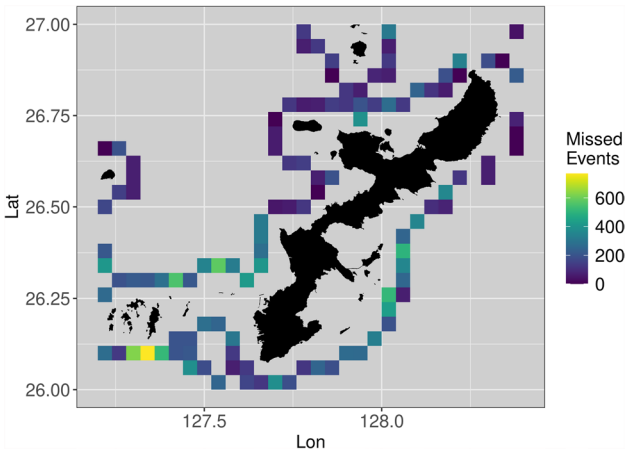

Fig. 8 Number of episodic chlor-*a* events across the 10-year time series (2011–2021) that were not detected at the commonly used 8-day 4-km ocean color grid resolution but that were captured by the 8×/day 500-m full-resolution GOCI grid configuration

(Wang et al. 2023). This critical increase in observational capacity facilitates a much better ability to monitor reef-adjacent habitat conditions and identify extreme events.

An important distinction to make in comparing polar-orbiting instruments with geostationary is the relative consistency in spatial resolutions. In a polar-orbit, even if a satellite nominally observes the Earth at a 750-m (VIIRS)/1-km (MODIS) spatial resolution, due to the variations in a satellite's viewing angle of the Earth as it collects data, pixels near the edge of a single scan can grow by a factor of 2 to 4, respectively (Wolfe et al. 2013). This effectively means that, for any given location on Earth, two consecutive days of satellite observations will have different spatial resolutions, sometimes drastically so. Thus, for operational consistency to monitor long-term trends, satellite data are usually binned to the lowest common resolution (e.g., 4 km), and this is the basis for the focused comparison of 500-m data against 4-km data in this analysis. By contrast, a geostationary sensor observes the Earth from the equator, meaning pixel size will grow as a function of latitude (Schaeffer et al. 2023), but will not change for a given location over the lifetime of the mission. This characteristic of a geostationary orbit makes it particularly well suited for monitoring applications, where coverage and consistency are optimized at the cost of losing global coverage. Other polar-orbiting satellites are designed to collect data at spatial resolutions at tens of meters (e.g., Landsat, Sentinel-2), which would also be very useful for coral reef applications, but these systems trade-off increased spatial information for infrequent revisit times, sometimes exceeding weeks before a satellite sees the same area twice.

High correlation between satellite ocean color-derived chlorophyll and K_d490 indices along reef habitat margins

It remains difficult to differentiate between water clarity and phytoplankton productivity from satellite ocean color even at higher spatial and temporal scales, in any given season, or during episodic high chlor-*a* events with the linear correlation matrix. The slopes of the linear relationships between K_d490 and chlor-*a* are lower and have a narrower range at the lowest spatial resolution. This suggests that because slopes are averaged out over space, they become reduced and less variable, which is likely why we see lower correlations at lower spatial resolutions. In this study we are assessing offshore waters along the reef margins where optical properties still derive largely from phytoplankton. Future work focusing on the development of GOCI water quality retrievals for shallow reefs where optical properties are influenced strongly by suspended sediments and dissolved organic matter could enhance our ability to differentiate between chlor-*a* and K_d490. This is exemplified by our finding that these optical properties begin to decouple during episodic events during which high levels of runoff may bring sediments and organic matter further offshore (Supplementary Fig. S5).

High empirical correlations exist between chlorophyll-a and light attenuation (K_d490) in oceanic waters where the light extinction is largely driven by phytoplankton biomass, or so-called Case 1 waters (Morel et al. 2007). The differences between chlorophyll-a concentration and K_d490 measured from the satellite observations are intrinsically small in clear waters when phytoplankton is the main driver of turbidity. Their differences become more prominent in turbid waters as well as waters of intermediate transparency when more complex algorithms were used to estimate K_d490 (Wang et al. 2009). In the reef-adjacent waters of coastal Okinawa Island, a decoupling between chlorophyll-a and K_d490 likely only occurs during short-lived episodic high turbidity events, e.g., runoff from land after heavy precipitations, or industrial/residential discharges. However, it remains difficult to distinguish the two satellite-derived parameters even during episodic events with the linear correlation matrix (Supplementary Fig. S5). Future work is directed to examine the K_d490 and chlorophyll-a concentration during episodic events with different matrixes, as well as to combine additional observations, e.g., satellite-derived variables at the near-infrared band, to better identify the sources of such events, such as colored dissolved organic matter (CDOM), suspended sediments and/or high nutrient input. Regardless of causality, it is notable that the varying time scales observed in this analysis produced statistically significant differences, highlighting the importance of matching observational scales with the variability of the ecosystem (Mannocci et al. 2017).

Coastal chlorophyll blooms/events are much more frequent and localized than is discernible from coarse resolution satellite data

Two areas that appear to experience the highest number of episodic extreme chlor-*a* events around Okinawa are near Nakagusuku Bay to the southeast and Naha to the southwest. Nakagusuku Bay is known to have polluted sediments due to large amounts of agriculture in the area. Naha is the capital city of Okinawa and holds the highest population density within the prefecture (*Japan: Administrative Division (Prefectures, Districts and Cities)—Population Statistics, Charts and Map*, n.d.), and is home to Tomari and Naha ports which are known to have polluted sediments due to shipping activity to and from these ports (Noah and Oomori 2006). Thus, heavy rainfall or other events causing runoff could lead to significantly enhanced production and turbidity around the reefs in the Naha region. However, at the lowest spatiotemporal resolutions these events are largely missed near Nakagusuku Bay. Knowing the precise areas impacted by potential runoff events is essential for targeted monitoring and management of reefs that could be negatively impacted by frequent exposure to polluted sediments.

Existing satellite grid configurations miss a substantial number of episodic events around the Kerama Islands. The Kerama Islands southwest of Okinawa are designated as Keramashoto National Park, a protected area that attracts a significant amount of reef-based tourism. The reefs of Keramashoto are a particularly important habitat for *Acropora sp.*, and this region acts as a key source of coral larvae for surrounding areas (Abe et al. 2021). Relying on low resolution satellite ocean color data to assess the water quality around Okinawa reefs may lead to completely overlooking this critical coral habitat.

The number of ocean color observations obtained by satellites can vary significantly during different seasons due in part to changes in the number of daylight hours. This partially explains why we found greater overall detections of episodic events during the summer months across all spatiotemporal grid resolutions, with ~3× more observations during the summer at the daily and 8×/day temporal resolutions despite the impacts from cloud cover during the rainy season. As summer is generally the rainy season in the Okinawa region, it is also likely that there is a true increase in the number of events occurring during the summer months. Nevertheless, while higher resolution data such as GOCI clearly increases the likelihood of capturing extreme events, this benefit to monitoring coral reef habitats may be significantly greater during the summer months, and wintertime monitoring may remain somewhat limited from remote sensing alone.

A limitation we encountered in this work was finding that the currently available bathymetry products (e.g., NOAA, GEBCO, SRTM) all differ slightly and do not identify the same shallow reef regions around Okinawa that are observed by satellite imagery as shown on Google Earth. Thus, it is possible that certain regions with high numbers of episodic events are influenced by shallow bathymetry that was incidentally retained during the shallow water masking process. However, these potentially contaminated shallow reef areas appear to represent only a small fraction of the overall region, and the majority of episodic events identified around Okinawa are reflective of ocean color properties not influenced by seafloor reflectance. Another challenge of this work was having limited access to in situ data to cross-validate the episodic events that were detected through satellite ocean color data. Future work could incorporate additional data sources, such as high-resolution precipitation data, to further investigate the timing of and conditions present during these episodic events. Nevertheless, high-resolution ocean color satellite data allows us to assign much more reliable risk to coral reef tracts in the tropical Pacific that could be affected by more frequent episodic events. It also allows us to assess the persistence of episodic events and manage these regions for coral restoration accordingly.

Implications for monitoring and risk assessment in reef habitat

Coral reef ecosystem processes, such as nitrogen fixation or decomposition, and animal waste products, such as reef-associated fishes can lead to increases in phytoplankton biomass near island- and atoll-reef ecosystems. This so-called island mass effect (IME) is found to be a feature among a majority of Pacific island- and atoll-reef ecosystems (Gove et al. 2016). High primary productivity is generally expected to benefit fisheries production and potentially provides favorable conditions for corals. For example, Gove et al. (2023) found that enhanced primary productivity supports herbivorous fish production, which facilitates coral growth by removing fleshy algae, and supports a positive feedback that promotes habitat suitability for reef fishes. However, we note that it is impossible from our study to differentiate the relative role of benthic-pelagic coupling that leads to production overflowing past ~30 m depth (such as tidal flushing of bays and back-reef) versus terrigenous inputs that lead to enhanced production both over the reef (i.e., <30 m of water) and offshore.

The ocean is a relatively dark target as viewed from space, making up only $\leq 10\%$, of the light signal seen from a satellite's perspective above the atmospheric layers. As such, ocean color satellite sensors need to be very sensitive in order to collect a usable signal, but not so sensitive that the radiance (light) signal saturates the optics. There are various trade-offs to consider that impact the potential usability of data products depending on the application. In

this study, we demonstrate the advantages of a geostationary orbit, which can "stare" at locations longer to build up a robust spectral signal with high signal to noise, and revisit a location multiple times per day, creating a sequence of images to mitigate cloud cover, as well as examine rates and fluxes. Having one instrument offer multiple observations also holds the advantage of having only one system to calibrate, as sensor-to-sensor disparities can create challenges in deriving consistent long-term biogeochemical trends (Welch et al. 2019). The trade-off with a geostationary orbit is that it can only view a particular portion of the globe over a mission lifetime, and spatial resolution generally does not exceed ~ 250 m due to mass constraints.

By contrast, using the Planet Dove satellite constellation (spatial resolution of 3 m and ~ 1-day revisit time), Sakuma et al. (2021) were able to demonstrate the utility of using very-high-resolution data for monitoring a short-lived sediment plume in coral reef areas of Kumejima Island, a small island near Okinawa. Having two orders of magnitude increase in spatial resolution at 1–2 day frequency is possible due to the nature of the Planet Dove constellation, which is comprised of "swarms" of nanosatellites with global coverage. While the demonstrated challenges associated with cloud cover still persist at this temporal frequency, satellites such as these offer a means of adding additional, more localized context to water quality events. The trade-off with nanosatellite constellations is that they generally exhibit a lower signal to noise ratio (3.5× lower than GOCI, and > 10× lower than satellites like MODIS and PACE), bringing potentially significant uncertainties to more quantitative assessments of biogeochemical parameters. This is additionally complicated by absolute radiometric uncertainties that are generally an order of magnitude higher (5–6% for Planet Dove at top of atmosphere) than for advanced satellites designed for ocean color (< 0.5% at top of atmosphere; Meister et al. 2011). Since the contribution of water-leaving reflectance to top of atmosphere reflectance is ≤ 10%, a 5–6% top of atmosphere radiometric uncertainty effectively translates to 50–60% uncertainty in water-leaving reflectance. Nevertheless, as satellites continue to approach the limits of quantum physics, it becomes evident that the most effective means of remote monitoring can be achieved by pairing different types of observations to leverage their respective strengths and weaknesses.

The use of hyperspectral satellite ocean color reflectance data can enable discernment of phytoplankton taxonomic resolution (Kramer et al. 2022; Cetinic et al. 2024), and the potential to assess and validate this capability on global scales is underway with the recent launch of NASA's Plankton, Aerosol, Cloud, and ocean Ecosystem (PACE) instrument (Gorman et al. 2019). Future satellites such as the Geostationary Littoral Imaging and Monitoring Radiometer (GLIMR, launching ~ 2028) and the Geostationary Extended Observations (GEO-XO, launching ~ 2032) mission (Dierssen et al. 2023; Lindsey et al. 2024) will further enable high spatial (300–500 m), high temporal (6–8× per day), hyperspectral information of phytoplankton community composition, representing the first ocean color geostationary satellites in the Western Hemisphere. These advancements in ocean color remote sensing technologies can improve our ability to more accurately describe water productivity and its relationship with the ecosystem, as well as to potentially help disentangle biological and water optical parameters.

Acknowledgements We would like to acknowledge Menghua Wang and Seung-Hyun Son of NOAA NESDIS STAR for providing the GOCI ocean color satellite data used in the study. We also thank Jamison Gove for his input on shallow water masking techniques and Thomas Oliver for his input on the relevance of this study to coral reef ecosystems. We thank Kisei Tanaka for his assistance with grid manipulation and for reviewing an early version of this manuscript, and we thank Dax Matthews for providing general satellite expertise and contributing bathymetry figures for this manuscript. We also acknowledge Guangming Zheng for providing input on satellite ocean color algorithms. Finally, we are thankful for the financial support provided by the NESDIS Geostationary Operational Environmental Satellites program and the NESDIS Center for Satellite Applications & Research.

Author contributions JNP led data analysis and manuscript writing for this project. HS, RRR, and JJS developed the project design and secured funding. HS, RRR, JJS, RAV, and DM contributed to manuscript writing, editing, and analysis feedback.

Data availability GOCI data are available through NESDIS (per request) and R code used for the analyses are available on GitHub (https://github.com/jnperelm/GOCI).

Declarations

Competing interests The authors declare no competing interests.

References

Abdelrhman MA (2017) Quantifying contributions to light attenuation in estuaries and coastal embayments: application to Narragansett Bay, Rhode Island. Estuaries Coasts 40:994–1012

Abe H, Kumagai NH, Yamano H, Kuramoto Y (2021) Coupling high-resolution coral bleaching modeling with management practices to identify areas for conservation in a warming climate: Kerama-shoto National Park (Okinawa Prefecture, Japan). Sci Total Environ 790:148094. https://doi.org/10.1016/j.scitotenv.2021.148094

Andrew NL, Bright P, de la Rua L, Teoh SJ, Vickers M (2019) Coastal proximity of populations in 22 Pacific Island Countries and Territories. PLoS ONE 14(9):e0223249

Asanuma I, Zhang X, Zhao C, Huang B, Hasegawa D (2014) Nutrients distribution in the coastal water of East Asia relative to the Kuroshio. Landscape Ecol Eng 10:191–199

Barnes BB, Hu C, Schaeffer BA, Lee Z, Palandro DA, Lehrter JC (2013) MODIS-derived spatiotemporal water clarity patterns in optically shallow Florida Keys waters: a new approach to remove bottom contamination. Remote Sens Environ 134:377–391

Bissett WP, Arnone RA, Davis CO, Dickey TD, Dye D, Kohler DD, Gould Jr RW (2004) From meters to kilometers: a look at ocean-color scales of variability, spatial coherence, and the need for fine-scale remote sensing in coastal ocean optics. Oceanography 17(2)

Brando VE, Dekker AG, Park YJ, Schroeder T (2012) Adaptive semi-analytical inversion of ocean color radiometry in optically complex waters. Appl Opt 51(15):2808–2833

Bryant D, Burke L, McManus JW, Spalding M (2001) Reefs at risk: a map-based indicator of threats to the world's coral reefs. SPC Women Fish 8:27–27

Cetinić I, Rousseaux CS, Carroll IT, Chase AP, Kramer SJ, Werdell PJ et al (2024) Phytoplankton composition from sPACE: requirements, opportunities, and challenges. Remote Sens Environ 302:113964

Choat JH, Clements KD, Robbins AW (2002) The trophic status of herbivorous fishes on coral reefs: 1: dietary analyses. Mar Biol 140:613–623

Choi J, Park YJ, Ahn JH, Lim H, Eom J, Ryu J (2012) GOCI, the world's first geostationary ocean color observation satellite, for the monitoring of temporal variability in coastal water turbidity. J Geophys Res Oceans 117(C9)

Couch CS, Oliver TA, Dettloff K, Huntington B, Tanaka KR, Vargas-Ángel B (2023) Ecological and environmental predictors of juvenile coral density across the central and western Pacific. Front Mar Sci 10:1192102

Devlin MJ, Petus C, Da Silva E, Tracey D, Wolff NH, Waterhouse J, Brodie J (2015) Water quality and river plume monitoring in the Great Barrier Reef: an overview of methods based on ocean colour satellite data. Remote Sens 7(10):12909–12941

Dierssen HM, Gierach M, Guild LS, Mannino A, Salisbury J, Schollaert Uz S et al (2023) Synergies between NASA's hyperspectral aquatic missions PACE, GLIMR, and SBG: opportunities for new science and applications. J Geophys Res Biogeosci 128(10):e2023JG007574

Doerffer R, Schiller H (2007) The MERIS Case 2 water algorithm. Int J Remote Sens 28(3–4):517–535

EPA (2022) https://www.epa.gov/coral-reefs/basic-information-about-coral-reefs

Geiger EF, Heron SF, Hernández WJ, Caldwell JM, Falinski K, Callender T, Greene AL, Liu G, De La Cour JL, Armstrong RA (2021) Optimal spatiotemporal scales to aggregate satellite ocean color data for nearshore reefs and tropical coastal waters: Two case studies. Front Mar Sci 8:643302

Gholizadeh MH, Melesse AM, Reddi L (2016) A comprehensive review on water quality parameters estimation using remote sensing techniques. Sensors 16(8):1298

Gorman ET, Kubalak DA, Patel D, Mott DB, Meister G, Werdell PJ (2019) The NASA Plankton, Aerosol, Cloud, ocean Ecosystem (PACE) mission: an emerging era of global, hyperspectral Earth system remote sensing. 11151, 78–84

Gove JM, Williams GJ, McManus MA, Heron SF, Sandin SA, Vetter OJ, Foley DG (2013) Quantifying climatological ranges and anomalies for pacific coral reef ecosystems. PLoS ONE 8(4):e61974

Gove JM, Williams GJ, Lecky J et al (2023) Coral reefs benefit from reduced land–sea impacts under ocean warming. Nature 621(7979):536–542

Gove JM, McManus MA, Neuheimer AB, Polovina JJ, Drazen JC, Smith CR, Merrifield MA, Friedlander AM, Ehses JS, Young CW, Dillon AK, Williams GJ (2016) Near-island biological hotspots in barren ocean basins. Nat Commun 7(1):Article 1

Hedley JD, Roelfsema CM, Chollett I, Harborne AR, Heron SF, Weeks S, Skirving WJ, Strong AE, Eakin CM, Christensen TRL, Ticzon V, Bejarano S, Mumby PJ (2016) Remote sensing of coral reefs for monitoring and management: a review. Remote Sens 8(2):118

Hoegh-Guldberg O, Poloczanska ES, Skirving W, Dove S (2017) Coral reef ecosystems under climate change and ocean acidification. Front Mar Sci 4:158

IOCCG (1999) Status and Plans for Satellite Ocean-Colour Missions: Considerations for Complementary Missions. In: Yoder JA (ed) Reports of the International Ocean-Colour Coordinating Group, No. 2, IOCCG, Dartmouth, Canada

IOCCG (2000) Remote Sensing of Ocean Colour in Coastal and Other Optically-Complex Waters; Report No. 3; IOCCG: Dartmouth, NS, Canada

Koba M (1992) Influx of the Kuroshio Current into the Okinawa Trough and inauguration of Quaternary coral-reef building in the Ryukyu Island Arc, Japan. Quat Res (Daiyonki-Kenkyu) 31(5):359–373

Kramer SJ, Siegel DA, Maritorena S, Catlett D (2022) Modeling surface ocean phytoplankton pigments from hyperspectral remote sensing reflectance on global scales. Remote Sens Environ 270:112879

Lee Z, Carder KL (2002) Effect of spectral band numbers on the retrieval of water column and bottom properties from ocean color data. Appl Opt 41(12):2191–2201

Lindsey DT, Heidinger AK, Sullivan PC, McCorkel J, Schmit TJ, Tomlinson M, Vandermeulen R, Frost GJ, Kondragunta S, Rudlosky S (2024) GeoXO: NOAA's future geostationary satellite system. Bull Am Meteorol Soc 105(3):E660–E679

Link JS, Watson RA (2019) Global ecosystem overfishing: Clear delineation within real limits to production. Sci Adv 5(6):eaav0474

Maina JM (2011) Global gradients of coral exposure to environmental stresses and implications for local management. PLoS ONE

Mannocci L, Boustany AM, Roberts JJ, Palacios DM, Dunn DC, Halpin PN et al (2017) Temporal resolutions in species distribution models of highly mobile marine animals: recommendations for ecologists and managers. Divers Distrib 23(10):1098–1109

McClanahan TR, Schroeder RE, Friedlander AM, Vigliola L, Wantiez L, Caselle JE, Graham NA, Wilson S, Edgar GJ, Stuart-Smith RD (2019) Global baselines and benchmarks for fish biomass: comparing remote reefs and fisheries closures. Mar Ecol Prog Ser 612:167–192

McKinna LI, Fearns PR, Weeks SJ, Werdell PJ, Reichstetter M, Franz BA et al (2015) A semianalytical ocean color inversion algorithm with explicit water column depth and substrate reflectance parameterization. J Geophys Res Oceans 120(3):1741–1770

McKinna LI, Werdell PJ (2018) Approach for identifying optically shallow pixels when processing ocean-color imagery. Opt Express 26(22):A915–A928

Meister G, McClain CR, Ahmad Z, Bailey SW, Barnes RA, Brown S, Werdell PJ (2011) Requirements for an advanced ocean radiometer (No. GSFC. TM. 5375.2011)

Morel A, Huot Y, Gentili B, Werdell PJ, Hooker SB, Franz BA (2007) Examining the consistency of products derived from various ocean color sensors in open ocean (Case 1) waters in the perspective of a multi-sensor approach. Remote Sens Environ 111(1):69–88

Noah NM, Oomori T (2006) Evaluation of Heavy Metal Pollution on the Coastal Marine Environments of Okinawa Island, Japan

Reichstetter M, Fearns PRCS, Weeks SJ, McKinna LIW, Roelfsema C, Furnas M (2015) Bottom reflectance in ocean color satellite remote sensing for coral reef environments. Remote Sens 7(12):Article 12

Russell BJ, Dierssen HM, Hochberg EJ (2019) Water column optical properties of pacific coral reefs across geomorphic zones and in comparison to offshore waters. Remote Sens 11(15):1757

Sakuma A, Abe H, Yamano H (2021) Short-term sediment plume event in the coral reef area of a small island captured by the Planet Dove satellite constellation. Remote Sens Lett 12(10):1038–1048

Schaeffer BA, Whitman P, Vandermeulen R, Hu C, Mannino A, Salisbury J et al (2023) Assessing potential of the Geostationary Littoral Imaging and Monitoring Radiometer (GLIMR) for water quality monitoring across the coastal United States. Mar Pollut Bull 196:115558

UNEP-WCMC, WorldFish Centre, WRI, TNC (2021) Global distribution of warm-water coral reefs, compiled from multiple sources including the Millennium Coral Reef Mapping Project. Version 4.1. Includes contributions from IMaRS-USF and IRD (2005), IMaRS-USF (2005) and Spalding et al. (2001). Cambridge (UK): UN Environment World Conservation Monitoring Centre

Wang M, Shi W (2006) Cloud masking for ocean color data processing in the coastal regions. IEEE Trans Geosci Remote Sens 44(11):3196–3105

Wang M, Son S, Harding Jr LW (2009) Retrieval of diffuse attenuation coefficient in the Chesapeake Bay and turbid ocean regions for satellite ocean color applications. J Geophys Res Oceans 114(C10)

Wang M, Ahn J-H, Jiang L, Shi W, Son S, Park Y-J, Ryu J-H (2013) Ocean color products from the Korean Geostationary Ocean Color Imager (GOCI). Opt Express 21(3):3835–3849. https://doi.org/10.1364/OE.21.003835

Wang M, Shi W, Jiang L (2023) Characterization of ocean color retrievals and ocean diurnal variations using the Geostationary Ocean Color Imager (GOCI). Int J Appl Earth Obs Geoinf 122:103404

Welch H, Hazen EL, Bograd SJ, Jacox MG, Brodie S, Robinson D et al (2019) Practical considerations for operationalizing dynamic management tools. J Appl Ecol 56(2):459–469

Werdell PJ, Franz BA, Bailey SW, Feldman GC, Boss E, Brando VE et al (2013) Generalized ocean color inversion model for retrieving marine inherent optical properties. Appl Opt 52(10):2019–2037.

Winston M, Oliver T, Couch C, Donovan MK, Asner GP, Conklin E et al (2022) Coral taxonomy and local stressors drive bleaching prevalence across the Hawaiian Archipelago in 2019. PLoS ONE 17(9):e0269068

Wolfe RE, Lin G, Nishihama M, Tewari KP, Tilton JC, Isaacman AR (2013) Suomi NPP VIIRS prelaunch and on-orbit geometric calibration and characterization. J Geophys Res Atmos 118(20):11–508.